1 23

Magnetic Field Modelling of a Soft Three-Axis Force Sensor

Damith Suresh Chathuranga, *Student Member, IEEE,* Zhongkui Wang, Yohan Noh, *Member, IEEE,* Thrishantha Nanayakkara, *Member, IEEE,* and Shinichi Hirai, *Member, IEEE,*

***Abstract*—This paper describes the modelling of a soft three axis force sensor. The sensor has a cylindrical cantilever beam made of silicone rubber that compress and bend when normal and tangential forces are applied. The displacement of the beam's end is calculated by measuring the change of the magnetic field emitted by a permanent magnet embedded in the soft beam. Spring theory and bending theory, are used to calculate the normal and tangential force components. The normal forces calculated by the proposed model and the measured values has an error less than 5% validating the analogy of the sensor to a soft cantilever beam under compression and bending. The proposed mathematical model is simple and faster than a finite element model, and accurately represents the non-linear behavior of the sensor's physical effects to applied loads.**

***Index Terms*—Force sensor, Magnetic field measurement, Modelling, Soft embodiment.**

I. INTRODUCTION

THE development of soft sensors and transducers has become a research trend in recent years. This growth is mainly due to the interest in developing soft robots [1], haptic devices [2], wearable electronics [3], medical instrumentations [4]-[5], and many other applications that require conformation of the sensor or transducer to different shapes. These applications need soft sensors that are accurate, robust, impact resistant, chemically inert, and inexpensive, instead of the bulky, rigid and expensive sensors that are presently available. Currently, research is being conducted to develop soft sensors that sense and measure different modalities such as force [6], pressure [7], strain [8], shear [9], proximity [10], and temperature [11]-[12]. In this paper, we focus our study on a sensor (Fig. 1) that measure forces along three axis. The sensor will be used to develop robotic tactile systems.

Commercially available force and tactile sensors mostly utilize structures such as beams and columns for sensing force. A structure is deformed under the external force, and the deformation in terms of stress, strain, displacement or pressure is measured using different types of transducers such as strain gauges, conductive ink, piezoelectric crystals, pressure gauges, light intensity, and magneto-elastic devices. Soft force sensors, on the other hand, use the same transduction principles yet are made of soft materials such as plastic [14], silicone [15], yarn and fabrics [16]. Table I contains a summary of soft sensors that measure force and stresses made from soft materials and utilize different transduction principles. The advantages of these sensors are that they are small, inexpensive and withstand impulse loads and loads that are much larger than the rated values. The downsides of these sensors are the none-linear behavior of measurements, higher hysteresis values, and inconsistency of the readings [16]. These problems can be reduced significantly by correctly modelling the sensor output. If the behavior of the soft embodiment is correctly predicted, the relationship between the measured value and the sensor output can be derived and used as the characteristic curves for the soft sensor. These information can be used to decide the sensor parameters, operational range, signal filters and methods to linearise the measured values.

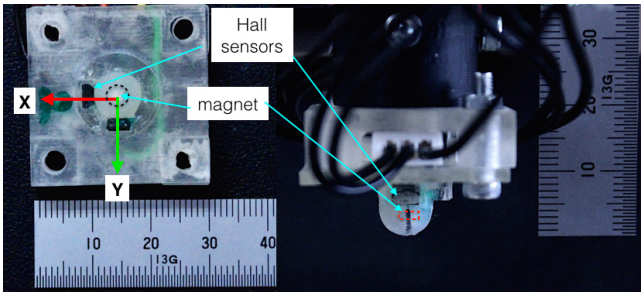

Fig. 1. Force sensor with a soft element covering a permanent magnet. The soft element is cylindrical and has a hemisphere at the end of the beam. Three Hall sensors are orthogonally placed around the soft element.

This paper introduces modelling of a three dimensional force sensor. The sensor has a soft cylindrical beam element that compresses and bends when a force is applied to the free end of the beam. A niobium permanent magnet is embedded inside the cylinder. The displacement of the beam's free end is calculated by measuring the change of the magnetic field emitted (using Hall sensors) by the magnet. The first mention of using Hall sensors for magnetic field measurement regarding development of tactile sensors was by Clark [36] and Nowlin [37]. In those studies, prototypes were presented. Next, Torres-Jara [38], Jamone [39]-[40], Ledermann [33], and Youssefian [41] presented sensors employing the same principle. Though these sensors essentially utilize the same sensing concept, the design of the sensors and the characterization of each sensor differ from our proposed sensor. The sensors proposed in the above papers defer mainly because they have a hollow cavity ,making it difficult to withstand loads much larger than the

Manuscript received March 30, 2016. This research was supported in part by JSPS Grant-in-Aid for Scientific Research 15H02230.

D. S. Chathuranga, Z. Wang and S. Hirai are with the Department of Robotics, School of Engineering, Ritsumeikan University, Shiga, Japan. e-mail: gr0120pr@ed.ritsumei.ac.jp, wangzk@fc.ritsumei.ac.jp, hirai@se.ritsumei.ac.jp

Y. Noh, and T. Nanayakkara is with Departmet of Informatics, King's College London, UK. e-mail: yohan.noh@kcl.ac.uk, thrish.antha@kcl.ac.uk

TABLE I
SOFT TACTILE SENSORS EMPLOYING DIFFERENT TRANSDUCTION PRINCIPLES TO SENSE FORCE, STRAIN AND STRESS.

Sensing modality	Transduction principle	Examples	Ability to detect dynamic forces (vibrations)
Force	Resistivity	strain gauges [18]	N/A
		fabric [16]	sample rate 100 Hz
		organic semiconductor [19]	N/A
		piezoresistance/MEMS [20], [21], [22]	sample rate 100 Hz
		Quantum Tunnelling Composites (QTC) [23]	N/A
		Microfluidic channels [24]	sample rate 100 Hz
		Electromagnetic induction [25]	sample rate 1 kHz
	Light intensity	Fiber optic sensor [26]	N/A
Shear force	Capacitance	differential capacitance [27]	N/A
	Piezoelectric	polyvinylidene fluoride (PVDF) films [28]	detects vibrations
	Resistivity	Quantum Tunnelling Composites (QTC) [29],[30]	Can sense dynamic loads
	Light intensity	Photodiode [31]	sample rate 30 Hz
strain	Resistivity	microchannels filled with conductive liquids [32]	N/A
	Magnetics	Magnetic field measurement using Hall sensors [33]	N/A
stress	Ultrasonic	electric impedance of a piezoelectric resonator [34]	N/A
	Light intensity	photodiode [19]	N/A

rated value, and the Hall sensors are placed parallel to the permanent magnet. Our proposed sensor has solid embodiment and Hall sensors orthogonal to each other. This construction helps the sensor to calculate the magnet displacement in the 3D space, while the previous research focused only on one direction, except for [33]. Furthermore, compared to the previous sensor structures, the proposed sensors use a mathematical model that accurately analyzes the relationship between applied normal and tangential forces, the soft material deformation, change in the magnetic field due to movement of the magnet, and the induced voltage of Hall sensors.

Most of the soft force sensors presented in the literature were modelled using finite element analysis (FEA) [44], [48]. This is due to the complexity in the sensors physical effects (deformation of materials) [45], non-linear behaviour in properties of the sensor [46] and the complex geometric shapes utilized in the sensors [47]. There were only few examples of mathematical representations of soft sensors. Even then, most of the times the geometry of the sensors were simplified to a simple geometric shape. Van [49] represented a force sensor that had a hemispherical embodiment to a bundle of beams that compressed and bent due to normal and tangential forces. Zhang [50] used a cantilever beam based modeling approach to model a slip sensor.

In the current study, the sensor's mathematical modelling and its characterization was done by representing the sensor as a single cantilever beam compressed and bent under normal and tangential forces. This sensor was initially proposed in [35], and [43] as a tool for minimally invasive surgery, and a tactile sensor for material classification. This paper further elaborates on its design, construction and extends the modelling and characterization. In Section II the operating principle, and fabrication of the sensor are described. Section III explains the mathematical modelling of the sensor. Section IV discusses the results of the simulation and Section V states the experimental results obtained. Finally, the paper is concluded with a discussion of the variables influencing the sensor performance, and future work.

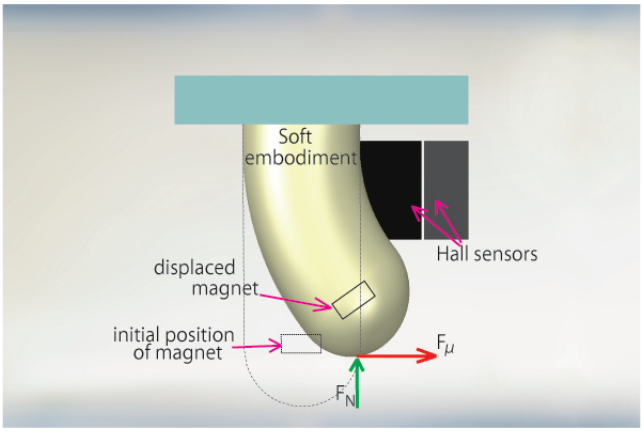

Fig. 2. Deformation of the soft embodiment due to normal (F_N) and tangential (F_μ) force.

II. SENSOR

A. Principle

The proposed sensor uses three Hall sensors that are orthogonally placed near a cylindrical soft beam made of silicone rubber. The free end of the beam was made as a hemisphere. A niobium permanent magnet is embedded in the silicone. When a force is applied to the free end of the cylinder, it is compressed and bent, displacing the magnet (see Fig. 2). This displacement causes changes in the magnetic field near the Hall sensors. By detecting these magnetic field changes, the position of the magnet is calculated. Next, trigonometry is used to calculate the displacement of the free end of the soft beam element. This deformation is analogues to a soft cantilever beam under compressive and bending force. Finally, using spring theory and bending theory, the normal and tangential force components are calculated.

B. Fabrication

The sensor is constructed with a soft sensing element fixed to a base (Fig. 3(a)). The base is made of ABS plastic using a 3D printer. Three Honeywell SS495A Hall sensors are fixed

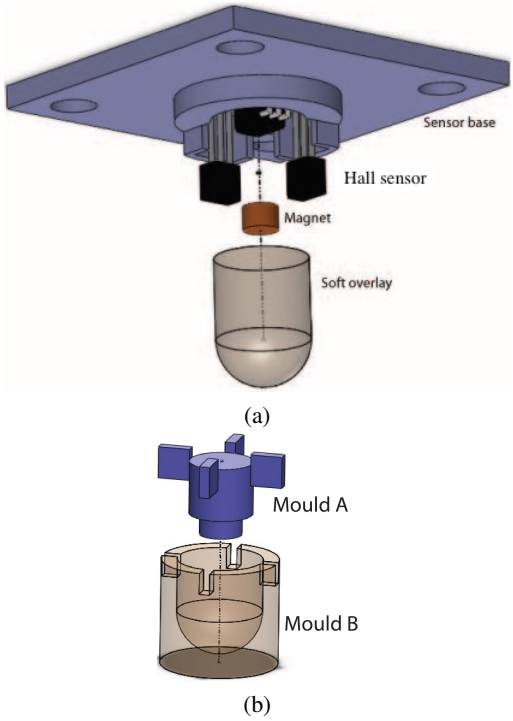

Fig. 3. (a) An exploded view of the sensor, (b) The molds used for making the soft element.

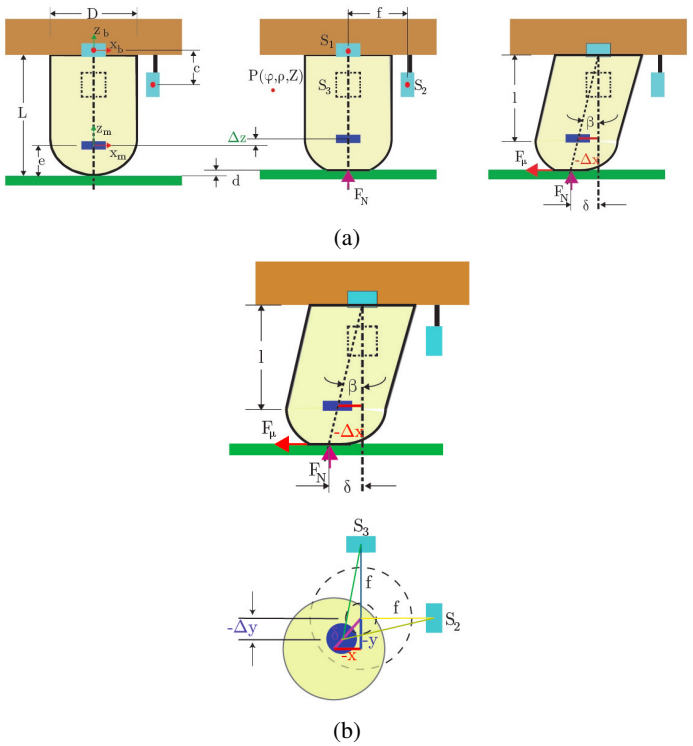

Fig. 4. (a) Coordinate system used for the calculation of the change in magnetic flux near the Hall sensors. The Hall sensors are perpendicular to each other, resulting in x, y, z orthogonal coordinates.X_b, Y_b, and Z_b are base coordinates, and X_m, Y_m, and Z_m are magnet coordinates. The sensor element is assumed to be a cylindrical cantilever beam element influenced by a horizontal and vertical load F_μ, F_N. (b) The end of the cylinder has a displacement of d, δ, while magnet has a displacement of $\Delta x, \Delta y$ and Δz.

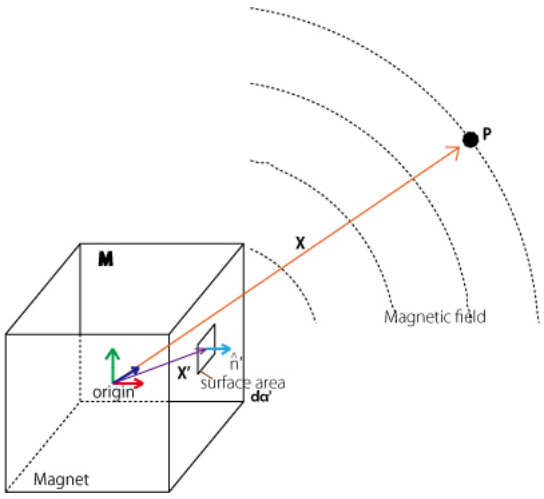

Fig. 5. Magnetic field induced by a magnet at point P.

to the base orthogonally to each other. The Hall sensors have directional sensitivity to magnetic flux. Therefore, the sensors are facing the center of the construction to ensure that a positive voltage change represents a positive change in the magnet displacement and a negative voltage change represents a negative displacement of the magnet in the x, y, or z direction.

The sensing element is made of a soft material (Smooth-on Dragon Skin 30) embedding a Niobium cylindrical magnet of diameter 4 mm. The outer layer of the sensing element is made using molds A and B (Fig. 3(b)). Mold A is inserted into mold B. Then, soft material mixture is poured in to the mold. Then, the mould is placed in a vacuum chamber (vacuum pressure 0.1 MPa) to remove the air bubbles. Next, the mold is held at a temperature of 80°C, for one hour in an oven to cure. Then, the part is removed from the oven, and mold A is removed. The magnet is inserted into the part, keeping the magnetic North down. The magnet is glued to the soft embodiment so that the soft body and magnet move together. Next, silicone rubber is used to cover the magnet and the cavity. The mold is placed again in the vacuum chamber and then, the oven. After the layers are formed, the molds are removed. Finally, the sensor base and the sensing element are fixed together using adhesive. It should be noted that the total price for the components of the sensor were not more than $20 making this construction inexpensive.

III. SENSOR MODELLING

The soft sensing element is a cylindrical cantilever with a diameter of D that has a hemispherical end (see Fig.4(a)). The length of the total element is L. The magnet was placed at the center of the hemisphere. The hemispherical end allows for the use of the assumption that an applied force on the surface will go through the center of the cylinder, where the magnet is placed, every time. Outside this soft element, the Hall sensors on the x, y directions were placed at a distance of f from the axis of the cantilever. When an external force was applied to the soft silicone hemisphere, the material deformed, displacing the magnet $\Delta x, \Delta y, \Delta z$. This caused the magnetic field to change near the Hall sensors. The magnetic field of a permanent magnet can be calculated from the vector potential: $\mathbf{B} = \nabla \times \mathbf{A}$,

where $\mathbf{A}$ is the magnetic potential. Let $\mathbf{M}$ be the volume magnetization of the magnet, $\hat{n'}$ be the unit vector normal to the surface area da' on the magnet at a location represented by position vector $\mathbf{X'}$, and μ_0 be the permeability of air (it is assumed that silicon rubber has the same permeability of air/vacuum). As shown in Fig. 5, the magnetic potential at arbitrary point P which is presented by position vector $\mathbf{X}$ is given by the following surface integral [42]

$$\mathbf{A} = \frac{\mu_0}{4\pi} \oint \frac{\mathbf{M}(\mathbf{X'}) \times \hat{n'}}{|\mathbf{X} - \mathbf{X'}|} da'. \tag{1}$$

This integral is performed over the entire surface of the magnet.

For a cylindrical magnet instead of using orthogonal coordinates X_m, Y_m, Z_m, cylindrical coordinates (α, R, z) is introduced for mathematical simplification. If cylindrical coordinate (ϕ, ρ, Z) represents the arbitrary point P (see Fig. 4(a)), equation 1 can be reduced to represent a magnetic field distribution A on a plane having an angle of ϕ with ρ axis as

$$A(\rho, Z) = \frac{\mu_0}{4\pi} M \iiint \frac{(z-Z) R \, \mathrm{d}R \, \mathrm{d}z \, \mathrm{d}\alpha}{\left[\rho^2 - 2R\rho\cos\alpha + R^2 + (z-Z)^2\right]^{3/2}}. \tag{2}$$

It can be noted that the magnetic flux is invariant along directional angle ϕ as a cylinder has symmetry around the axis. Therefore it is ignored in the calculations. Above equation can be simplified to the following to calculate the components of the magnetic field in z and R directions that represented by $A(Z)$, $A(\rho)$:

$$\begin{aligned} A(Z) = &- \frac{\mu_0}{4\pi} M \int_0^{2\pi} \int_0^{a} \frac{R(L/2 - z)}{\left[R^2 + (L/2-z)^2 + \rho^2 - 2R\rho\cos\alpha\right]^{3/2}} \\ &+ \frac{R(L/2 + z)}{\left[R^2 + (L/2+z)^2 + \rho^2 - 2R\rho\cos\alpha\right]^{3/2}} \, \mathrm{d}R \, \mathrm{d}\alpha \\ A(\rho) = &- \frac{\mu_0}{4\pi} M \int_0^{2\pi} \int_0^{a} - \frac{R(2\rho - 2R\cos\alpha)}{2\left[R^2 + (L/2-z)^2 + \rho^2 + 2R\rho\cos\alpha\right]^{3/2}} \\ &+ \frac{R(2\rho - 2R\cos\alpha)}{2\left[R^2 + (L/2+z)^2 + \rho^2 - 2R\rho\cos\alpha\right]^{3/2}} \, \mathrm{d}R \, \mathrm{d}\alpha \end{aligned} \tag{3}$$

where a is the radius of the magnet. Finally, the magnitude of the magnetic field in units of weber (Wb) at a given point can be calculated as:

$$B_{tot} = \sqrt{A(Z)^2 + A(\rho)^2} \tag{4}$$

1) Force Calculation: We assume that two forces F_N, F_μ are applied at the end of the cylinder. These forces are perpendicular to each other. Due to the tangential force F_μ, the cylinder bends δ at the end. When there is a relative motion, this bending force can be assumed to be equal to the friction force between the soft cylinder and the contact surface. The force F_N, which is normal to the contact surface, is compressing the soft cylindrical beam to a depth of d. We assume that the soft cylinder behaves like a cantilever elastic beam (Fig. 4(b)). We then write the compression and bending equations as follows:

$$F_N = \frac{EA}{L} d \tag{5}$$

The tangential force F_μ is calculated from the bending formula as:

$$F_\mu = 3EI \frac{\delta}{l^3}, \tag{6}$$

where A, E, L, I are the cross sectional area of beam, the Young's modulus of the soft material, the natural length of beam and the moment of inertia of the cross section of the cantilever beam. The cross sectional area of the cantilever beam is calculated as:

$$A = \pi \left[\left(\frac{D}{2}\right)^2 - \left(\frac{D}{2} - d\right)^2 \right], \tag{7}$$

where D is the diameter of the cantilever beam and d is the deformation of the contact point in the z direction.

2) Displacement Calculation: Due to the normal and tangential (frictional) force F_N, F_μ, the end of the soft cylinder moves x, y, d from the initial position, causing the magnet to move $\Delta x, \Delta y, \Delta z$. Then, from geometric relations we find:

$$\Delta x = \left[\frac{(L-d) - (\Delta z + e + d)}{(L-d)} \right] x,$$

$$\Delta y = \left[\frac{(L-d) - (\Delta z + e + d)}{(L-d)} \right] y,$$

$$\Delta z = l + d - e,$$

where e is the unstressed distance from the end of the cantilever beam to the center of the magnet. The coordinates of the Hall sensors (S_1, S_2 and S_3) can be written from the magnet coordinate system (ϕ, ρ, Z) for figure 4(b) as:

$$\begin{aligned} S_1 &: \quad (\phi_1, l, \sqrt{\Delta x^2 + \Delta y^2}) \\ S_2 &: \quad (\phi_2, l - c, \sqrt{\Delta y^2 + (f + \Delta x)^2}) \\ S_3 &: \quad (\phi_3, l - c, \sqrt{\Delta x^2 + (f + \Delta y)^2}) \end{aligned}$$

As the magnet has a symmetry around its z axis, the magnetic flux around axis at a distance of (ρ, Z) is the same for a given ϕ. Therefore, ϕ_1, ϕ_2, ϕ_3 are ignored in these calculations.

IV. SIMULATION RESULTS

In order to develop the look up table that contains magnetic field values induced near sensors 1, 2, and 3 for a given displacement of the magnet, a numerical simulation was carried out. The parameters for the Eqs. (3) and (4) are given in table II. Figure 6 represents the value of the magnetic fields near sensor 1 (Z direction), sensor 2 (X direction) and sensor 3 (Y direction) for the displacement in the horizontal directions and a contact depth $d = 1$ mm calculated by Eq. (3) and (4). Similarly, the magnetic field values for a contact depth d up

TABLE II
PARAMETERS FOR SIMULATION

Parameter	value
Diameter of cantilever beam (D)	8 mm
Length of cantilever beam (L)	9 mm
Distance of Hall sensors in directions x, y from z (f)	5 mm
Young's Modulud (E)	1 MPa
Volume magnetization (M)	1
Permeability - of air/vacuum (μ_0)	$4\pi \times 10^{-7}$ H/m

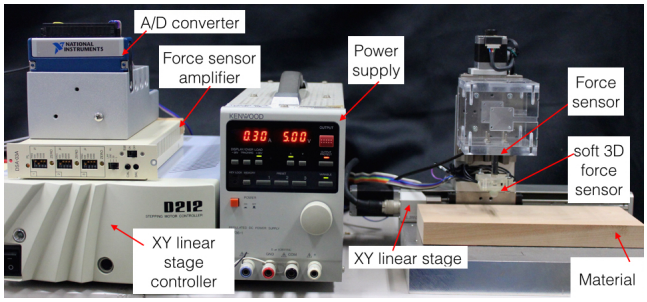

Fig. 7. Experimental setup

to 3 mm and horizontal displacements x, y between -3 mm to 3 mm were calculated and saved as a look up table. The values were conducted in steps of 0.01 mm.

From Fig. 6, it is noticed that if the magnet displaced in a 3D space, the set of magnetic field values near three sensors, are unique to each location. Therefore, if magnetic field at the three locations are matched with the above developed look up table, the displacement of the magnet, and then the displacement of the end of the cantilever beam can be calculated. Finally, the normal and tangential force is calculated using Eq. (5), and (6).

V. EXPERIMENTAL VALIDATION

A. Experimental setup

The experimental setup is shown in Fig. 7. The system consists of a soft tactile sensor rigidly fixed to the vertical linear stage of the XY table (Suruga Seiki KXL06100-C2-F) using a Tech Gihan (USL 06-H5-50N-C) force sensor. The vertically moveable linear stage is fixed to a horizontal linear stage. Both stages allow the tactile sensor to move in the x and z directions. The linear stages have a step size of 4 μm. The force sensor is capable of measuring the forces in three dimensions. The force sensor has an amplifier of its own, and the processed signal is sent to a National Instruments NI9205 analog to digital converter.

The linear stages and the AD converters are connected to a computer and controlled through LabView software. The data retrieval and the linear stage motion are synchronized by the software. The sampling rate of the AD converter is 1000 Hz. For most of the tests, the output signal is filtered using a 500 Hz cut off frequency low pass and an average filter.

From calibration tests, we found that Hall sensor has a conversion factor of 6.463×10^5 V/Wb (volts per weber). Therefore, by measuring the sensor's output voltage (offset

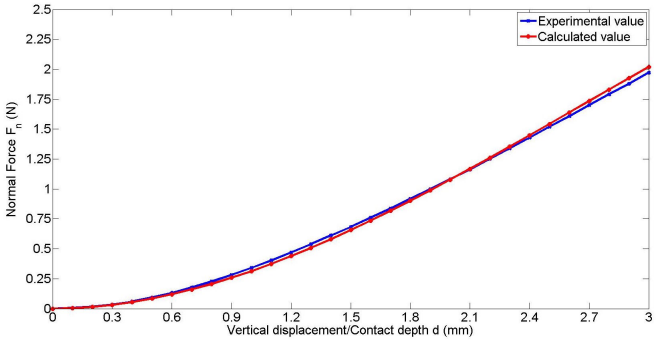

Fig. 8. Normal force F_N vs. z directional displacement

compensated), we could measure the magnetic flux induced by the magnet at the location of the sensor. The Hall sensor offset voltage was 2.87 V for sensor 1 and was subtracted from the sensor output voltage value. This offset value is unique to each sensor and depends on the Hall sensor and the initial distance of the sensor from the permanent magnet.

B. Experiments and Simulations

For the experiments, a normal force F_N was applied by pushing the soft tactile sensor onto a hard surface for a depth d. The sensor was stationary in the horizontal direction $(F_\mu = 0)$. After waiting for 30 s for the sensor value to settle, the force was measured using the force sensor. The displacement was measured using the encoders in the linear stage. The voltage output of the three Hall sensors $V_{S_x}, V_{S_y}, V_{S_z}$ were recorded for each step of the normal force F_N and the deformation d. The depth of the contact was changed with steps of 4 μm. The average of the voltages for the increase in depth and decrease in depth were calculated and saved in a table. Ten trials were carried out and the average values of these trials were taken for the calculations.

In order to validate the sensor behavior, numerical simulation values and experimental results were compared. Figure 8 represents the measured normal force F_N and the calculated normal force from the Eq. (5). The calculated values and the experimental values behaved similarly up to a contact depth of $d = 3$ mm. The contact depth of 3 mm was chosen as the limit. This was needed in order to limit the deformation of the soft material. The maximum error between the calculated and the actual force values was less than 5%. This suggest that for normal load calculations the assumption of an elastic beam under compression was valid.

Next, for a given normal force F_N, the displacement of the magnet in the z direction was calculated, and using Eq. (3), and (4), the magnetic field was calculated. Subsequently, this value was converted to sensor voltage by multiplying the magnetic field value by the Hall sensor conversion factor. The results of the normal force vs sensor voltage are presented in Fig. 9. It can be noted that the calculated voltage and the actual voltage have similar trends yet the deviation is increases with the normal load yet error was under 5% of the maximum measurement.

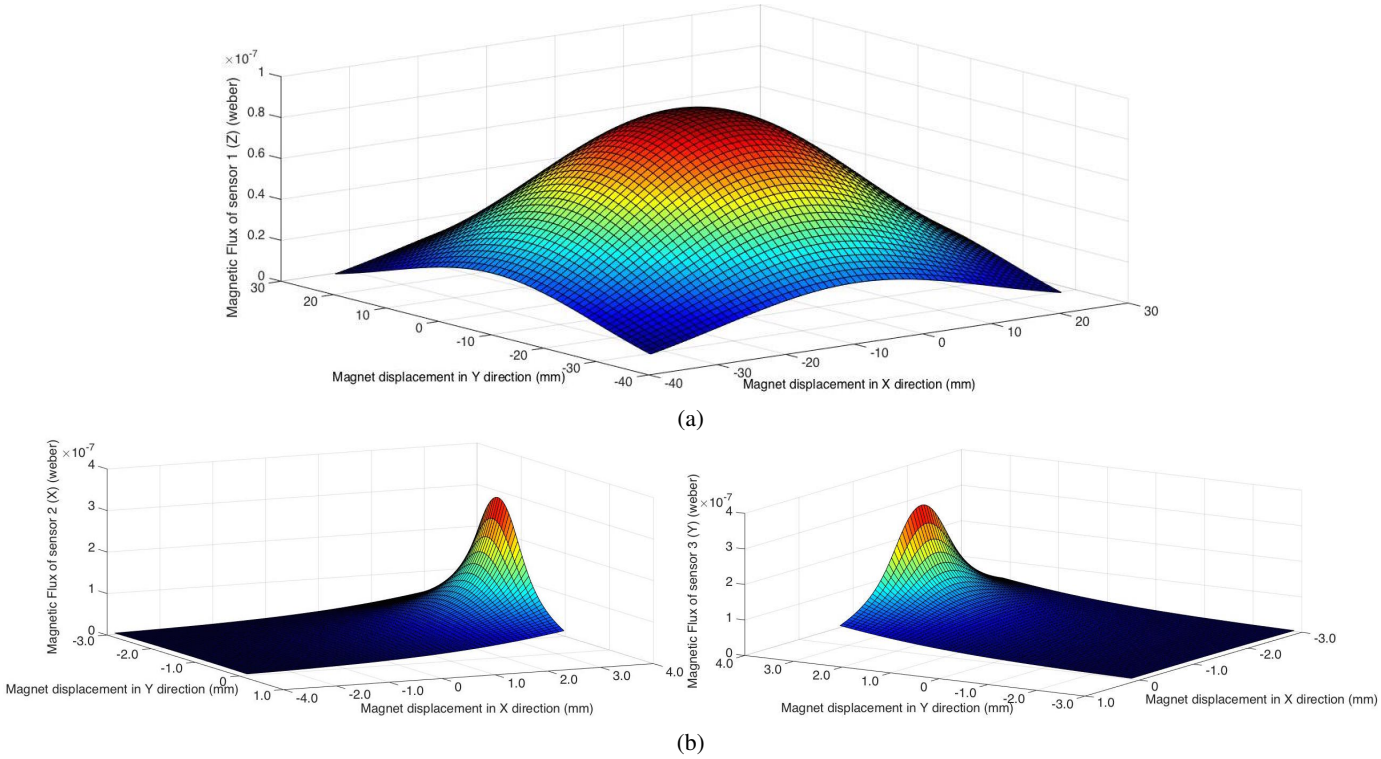

Fig. 6. Sensor values calculated from the above simulation (a) sensor 1 values for $x, y = -3:3$ mm, $z = 1$ mm (b) sensor 2, and sensor 3 values for $x, y = -3:3$ mm, $z = 1$ mm

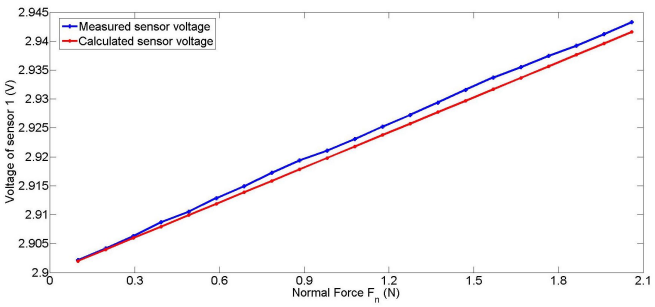

Fig. 9. Normal force F_N vs. sensor 1 voltage

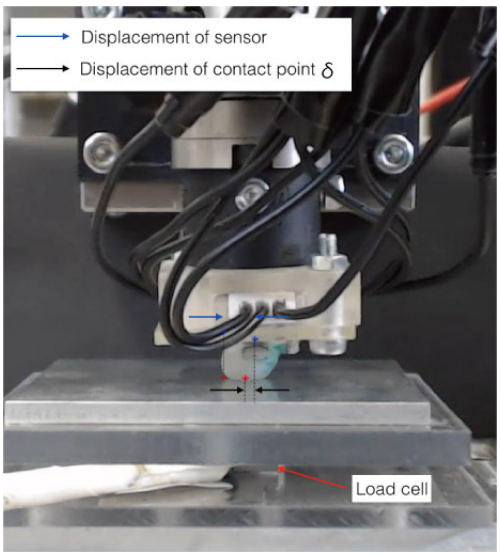

Fig. 10. Setup used for the calculation of the displacement in the horizontal direction. Displacement in the x direction δ is measured by processing the image and measuring the distance between the initial and final position of the feature point.

Similar to normal force F_N, the tangential force F_μ was calculated using Eq. (6). The actual horizontal force was measured using the force sensor that was fixed to the bottom contact surface (Fig. 10). The measurement of the horizontal deformation δ posed a problem, as this was affected by the frictional coefficient of the bottom contact surface and the slippage between the palate and the tactile sensor. Therefore, in order to obtain an relatively accurate result, the deformation caused by the dynamic frictional force at the moment of slipping was used. The deformation was measured by visual odometry (Fig. 10). Again, ten trials were conducted, and the average of the values were taken for the calculations.

Figure 11, shows the relationship between the horizontal displacement δ and the horizontal force F_μ. For a horizontal displacement of up to 3.1 mm, the simulated value and the actual values have similar trends. The measured force had an error much larger than expected. This error can be acceptable as this was an prototype system and the deformation of the beam could not be accurately measured from visual odometry.

C. Frequency response

In order for this sensor to be used as a tactile sensor in robotic hands, the sensor should be able to measure vibrations up to 500 Hz [13]. Thus, the sensor was subjected to vibrations

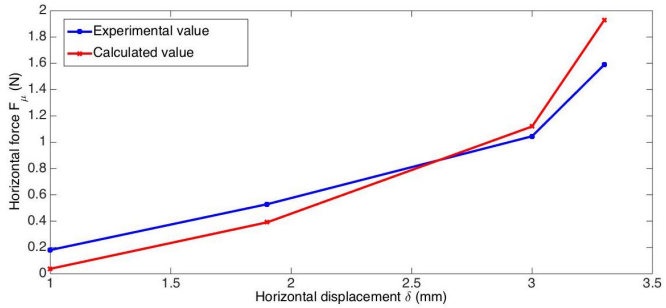

Fig. 11. Horizontal force F_μ vs. x directional displacement

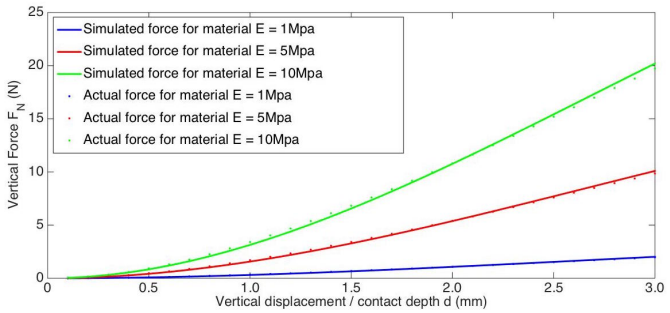

Fig. 12. Normal force F_N vs. z directional displacement for materials with different stiffness

of up to 600 Hz using a vibration table. The sensor was sensitive enough to sense vibrations up to and over 600 Hz. Calculations that used the principle of undamped natural frequency of a mass-spring system indicated that natural frequency of the sensor was approximately 970 Hz, which is above the sensor functioning region.

VI. DISCUSSION

This paper introduces the initial prototype of a soft force sensor and its modelling in order to calculate normal (F_N) and tangential (F_μ) force components. The deformation of the sensor's soft embodiment due to the above forces is calculated indirectly by measuring the magnetic field variation of a permanent magnet embedded in the soft embodiment. The magnetic field around the space of the magnet is calculated numerically and stored in the system as a lookup table. The magnetic field of three fixed locations are measured using Hall sensors. When the magnet displaces from its initial

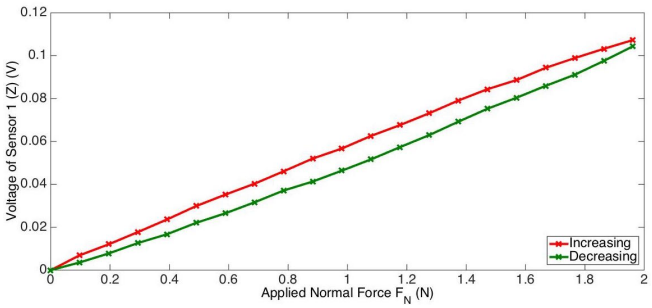

Fig. 13. Hysteresis of the sensor in the normal direction (Z)

location, the magnetic field values around the fixed locations change. The new magnetic field values are measured using the Hall sensors and the three value set is matched with the numerically calculated value set (lookup table) and the location of the magnet relative to the three fixed locations are retrieved. Next, using trigonometry, the displacement of the free end of the cylindrical soft embodiment is calculated. As the cylindrical embodiment is assumed as a cantilever beam under compressive and bending forces, using spring theory and bending theory, the normal F_N, and tangential F_μ force is calculated. Initially this calculations were carried out post process. The results show that the normal force F_N and tangential force or friction force F_μ can be measured using this sensor accurately. The force sensor has the ability to measure dynamic loads, making it suitable for tactile sensing applications. The proposed mathematical model describes the sensor behavior well. Therefore, the simulated results can be used in constructing the look up table for the sensor. This is an advantage compared to many other soft tactile sensors, where the mathematical representation of the sensor behaves differently than the actual sensor.

The sensitivity of the sensor depends on the stiffness of the soft material. As seen in Fig. 12, by changing the material, the sensitivity of the sensor can be changed. For a Young's modulus of $E = 1$ MPa, the maximum force that can be measured with an error less than 5% is 3.0 N, while for a modulus of 5 MPa, it is approximately 9 N. If the modulus is increased to 10 MPa, the maximum force measurable increases to approximately 18 N. Therefore, this sensor could be used to measure small and large forces just by changing the stiffness of the sensing element.

Figure 13 shows the maximum hysteresis of the sensor. The maximum hysteresis value is within 10% of the full scale value. The hysteresis of the sensor depends on the damping of the soft embodiment. In our calculations the soft material is assumed perfectly elastic having no damping. This assumption has made the calculations simple. The material selected showed minimum damping making the simulated and calculated values within acceptable range.

According to the Eq. (3), the magnetic field of a permanent magnet is dependent on the distance of the point. Additionally, as per the equations, it is noted that the both components $(A(\rho), A(Z))$ of the field calculation act significantly. To simplify the calculations, the orientation (yaw, pitch and roll) of the magnet is ignored. We believe that this assumption has led to most of the deviations in the magnetic flux calculations (see deviation in Fig. 11). Currently, the system does not include calculation of roll and pitch but if these components are added, the calculations will be more accurate. Additionally, the deviation in Fig. 11 can be caused by the error in measuring the horizontal displacement using visual odometer as the minimum displacement measurable was approximately 0.125 mm.

The concept of magnetic field measurement of a permanent magnet as the transduction principle has made the sensor robust. As the sensitive and fragile components (Hall sensors) are away from contacting with the external force, these components are safe from excessive loads. Additionally, as there are

no electrical connections inside the soft embodiment, sensor has the ability to deform and come to its initial shape after the forces are removed. Finally, the modular behavior of the components of the sensor make it easy to change the sensitivity (by changing the stiffness of the soft embodiment), easy to repair, and due to the use of inexpensive components, disposable. Therefore this sensor provides an inexpensive solution for bio-medical applications as well as robotic applications in tactile sensing.

VII. CONCLUSION

This paper presents the development of a mathematical model to a soft three axis force sensor. The prototype force sensor was assumed as a soft cantilever beam under a compressive and bending load. Normal force acting on the sensor was considered as the compressive force while the tangential force was considered as bending force. The displacement of the free end of the beam was obtained by analyzing magnetic field variations at three fixed locations due to the displacement of a permanent magnet which was embedded in the soft cantilever beam. Using spring theory and bending theory, the normal and tangential forces were calculated. The experiment results and simulation results were significantly similar to each other concluding that the assumptions made at the development of the sensor model were valid and the proposed analogy of the sensor soft embodiment to a compressive and a bent cantilever beam was valid. Furthermore, the simplification of the magnetic field calculations of a cylinder by removing the yaw, pitch and roll effects did not affect the accuracy of the normal force measurement of the sensor significantly. The modelling theory used in this paper shows promise in calculating forces accurately for a force sensor embodying a soft elastic element as the structure used for measuring forces applied normal and tangentially to the sensor.

REFERENCES

[1] Y. L. Park, B. Chen, C. Majidi, and R. J. Wood, "Active modular elastomer sleeve for soft wearable assistance robots," *IEEE/RSJ International Conference on Intelligent Robots Systems*, pp. 1595-1602, 2012.

[2] A. Okamura and M. Cutkosky, "Feature detection for haptic exploration with robotic fingers," *International Journal of Robotics Research*, vol. 20, no. 12, pp. 925-938, 2001.

[3] D. Marculescu, R. Marculescu, N. Zamora, P. Stanley-Marbell, P. Khosla, S. Park, S. Jayaraman, S. Jung, C. Lauterbach, W. Weber, T. Kirstein, D. Cottet, J. Grzyb, G. Troster, M. Jones, T. Martin, and Z. Nakad, "Electronic textiles: A platform for pervasive computing," *Proc. IEEE*, vol. 91, no. 12, pp. 1995-2018, 2003.

[4] P. Puangmali, K. Althoefer, L.D. Seneviratne, D. Murphy, and P. Dasgupta, "State-of-the-art in force and tactile sensing for minimally invasive surgery," *IEEE sensors Journal*, vol. 8, no. 4, pp. 371-381, 2008.

[5] T. Yamamoto, B. Vgvlgyi, K. Balaji, L. L. Whitcomb, and A.M. Okamura, "Tissue property estimation and graphical display for teleoperated robot-assisted surgery," *IEEE International Conference on Robotics and Automation*, pp.4239-4245, 2009.

[6] L. Viry, A. Levi, M. Totaro, A. Mondini, V. Mattoli, B. Mazzolai, and L. Beccai, "Flexible three-axial force sensor for soft and highly sensitive artificial touch," *Advanced Materials*, vol. 26, pp. 2659-2664, 2014.

[7] S. C. B. Mannsfeld, B. C-K. Tee, R. M. Stoltenberg, C. V. H-H. Chen,S. Barman, B. V. O. Muir, A. N. Sokolov, C. Reese and Z. Bao, "Highly sensitive flexible pressure sensors with microstructured rubber dielectric layers," *Nature Materials*, vol. 9, pp. 859-864, 2010.

[8] C. Cochrane, V. Koncar, M. Lewandowski and C. Dufour, "Design and Development of a Flexible Strain Sensor for Textile Structures Based on a Conductive Polymer Composite," *Sensors*, vol. 7, no.4, pp. 473-492, 2007.

[9] H. Lee, J. Chung, S. Chang, and E. Yoon, "Normal and sheer force measurement using flexible polymer tactile sensor with embedded multiple capacitors," *Journal of Microeletromechanical Systems*, vol. 17, no. 4, pp. 934-942, 2008.

[10] C. Wang, K. Huang, D. T. W. Lin, W. Liao, H. Lin and Y. Hu, "A Flexible Proximity Sensor Fully Fabricated by Inkjet Printing," *Sensors*, vol. 10, no. 5, pp. 5054-5062, 2010.

[11] M. Ahmed, M. M. Chitteboyina, D. P. Butler, and Z. C. Butler, "Temperature Sensor in a Flexible Substrate," *IEEE Sensors Journal*, vol. 12, no. 5, pp. 864-869, 2012.

[12] T. Someya, Y. Kato, T. Sekitani, S. Iba, Y. Noguchi, Y. Murase, H. Kawaguchi, and T. Sakurai, "Conformable, flexible, large-area networks of pressure and thermal sensors with organic transistor active matrixes," *Proc. of National Academy of Sciences of the USA*, vol. 102, no. 35, pp. 12321-12325, 2005.

[13] R.S. Dahiya, G. Metta, M. Valle and G. Sandini, "Tactile sensing-from humans to humanoids," *IEEE Transactions on Robotics*, vol.26, no. 1, pp. 1-20, 2010.

[14] S. Khan, S. Tinku, L. Lorenzelli and R. D. Dahiya, "Flexible tactile sensor using screen-printed p(VDF-TrFE) and MWCNT/PDMS composites," *IEEE sensors Journal*, vol. 15, no. 6, pp. 3146-3155, 2015.

[15] D. S. Chathuranga, V. A. Ho and S. Hirai, "Investigation of a biomimetic fingertip's ability to discriminate fabrics based on surface textures," *IEEE/ASME International Conference on Advance Intelligent Mechatronics*, pp. 1667-1674, 2013.

[16] V. A. Ho, D. Kondo, S. Okada, T. Araki, E. Fujita, M. Makikawa and S. Hirai, "Development of a Low-Profile Sensor Using Electro-conductive Yarns in Recognition of Slippage," *IEEE Int. Conf. on Intelligent Robots and Systems*, pp. 1946-1953, 2011.

[17] M. Jafaripanah, B. M. Al-Hashimi, and N. M. White, "Application of Analog Adaptive Filters for Dynamic Sensor Compensation," *IEEE Transactions on Instrumentation and Measurements*, vol. 54., no. 1, pp. 245-251, 2005.

[18] K. N. Tarchanidis, and J. N. Lygouras , "Data Glove With a Force Sensor," *IEEE Transactions on Instrumentation and Measurements*, vol. 52, no. 3, pp. 984-989, 2003.

[19] J. Missinne, E. Bosmanb, B. V. Hoea, R. Verplanckea, G. V. Steenbergea, S. Kalathimekkada, P. V. Daele, and J. Vanfleteren, "Two axis optoelectronic tactile shear stress sensor," *Sensors and Actuators A: Physical*, vol. 186, pp. 63-68, 2012.

[20] K. Kim, K. R. Lee, W. H. Kim, K. Park, T. Kim, J. Kim, and J. J. Pak, "Polymer-based flexible tactile sensor up to 32 32 arrays integrated with interconnection terminals," *Sensors Actuat. A, Phys.*, vol. 156, pp. 284-291, 2011.

[21] V. A. Ho, D. V. Dao, S. Sugiyama and S. Hirai, "Analysis of Sliding of a Soft Fingertip Embedded with a Novel Micro Force/Moment Sensor : Simulation, Experiment, and Application," *IEEE Int. Conf. on Robotics and Automation*, pp. 889-894, 2009.

[22] F. Boissieu. C. Godin, B. Guilhamat, D. David, C. Serviere and D. Baudois , "Tactile Texture Recognition with a 3-Axial Force MEMS integrated Artificial Finger," *Proc. Robotics: Science and Systems*, pp. 49-56, 2009.

[23] Y. W. R. Amarasinghe, A. L. Kulasekera, T. G. P. Priyadarshana, "Quantum Tunneling Composite (QTC) Based Tactile Sensor Array For Dynamic Pressure Distribution Measurement," *7th International Conference on Sensing Technology*, pp. 1-4, 2013.

[24] D. M. Vogt, Y. L. Park, and R. J. Wood, "Design and Characterization of a Soft Multi-Axis Force Sensor Using Embedded Microfluidic Channels," *IEEE sensors Journal*, vol. 13, no. 10, pp. 4056-4064, 2013.

[25] S. Takenawa, "A soft three-axis tactile sensor based on electromagnetic induction," *IEEE International Conference on Mechatronics*, pp.1-6, 2009.

[26] Y. Noh, S. Sareh, J. Back, H. A. Wrdemann, T. Ranzani, E. L. Secco, A. Faragasso, H. Liu, and K. Althoefer, "A Three-Axial Body Force Sensor for Flexible Manipulators," *IEEE/ASME International Conference on Robotics and Automation*, pp. 6388-6393, 2014.

[27] M. I. Tiwanaa, A. Shashankb, S. J. Redmondb, and N. H. Lovell, "Characterization of a capacitive tactile shear sensor for application in robotic and upper limb prostheses," *Sensors and Actuators A: Physical*, vol. 165, no. 2, pp. 164-12, 2011.

[28] K. Hosoda, Y. Tada, and M. Asada, "Anthropomorphic robotic soft fingertip with randomly distributed receptors," *Robot. Auton. Syst*., vol. 54, no. 2, pp. 104-109, 2006.

[29] T. Zhang, L. Jiang, X. Wu, W. Feng, D. Zhou and H. Liu, "Fingertip Three-Axis Tactile Sensor for Multifingered Grasping," *IEEE Transactions on Mechatronics*, vol. 20, no. 4, pp. 1875-1885, 2015.

[30] T. Zhang, H. Liu, L. Jiang, S. Fan and H. Liu, "Development of a Flexible 3-D Tactile Sensor System for Anthropomorphic Artificial Hand," *IEEE sensors Journal*, vol. 13, no. 2, pp. 510-518, 2013.

[31] J. Missinne, A. Monte, Y. Tijtgat, N. Rossey and G. V. Steenberge, "Miniature Multiaxial Optoelectronic Shear Stress Sensing System Based on a Segmented Photodiode," *IEEE sensors Journal*, vol. 15, no. 8, pp. 4286-4291, 2015.

[32] J. B. Chossat, Y. L. Park, R. J. Wood, and V. Duchaine, "A Soft Strain Sensor Based on Ionic and Metal Liquids," *IEEE Sensors Journal*, vol.13, no.9 pp. 3405-3414, 2013.

[33] C. Ledermann, S. Wirges,, D. Oertel, M. Mende and H. Woern, "Tactile sensor on a magnetic basis using novel 3D hall sensor - first prototypes and results," *IEEE 17th International conference on intelligent engineering systems*, pp. 55-60, 2013.

[34] K. Kim, S. Zhang, J. Tian, P. Han, and X. Jiang, "Face-shear mode ultrasonic tactile sensor array," *IEEE International Ultrasonics Symposium*, pp. 1059-1062, 2012.

[35] D. S. Chathuranga, Z. Wang, Y. Noh, T. Nanayakkara and S. Hirai, "Disposable Soft 3 Axis Force Sensor for Biomedical Applications," *The 37th Annual International Conference of the IEEE Engineering in Medicine and Biology Society (EMBS)*, 2015.

[36] J. J. Clark, "A magnetic field based compliance matching sensor for high resolution, high compliance tactile sensing," *in Proc. IEEE ICRA*, pp. 772-777, 1988.

[37] W. C. Nowlin, "Experimental results on Bayesian algorithms for interpreting compliant tactile sensing data," *in Proc. IEEE ICRA*, pp. 378-383, 1991.

[38] E. Torres-Jara, I. Vasilescu, and R. Coral, "A soft touch: Compliant tactile sensors for sensitive manipulation," Massachusetts Inst. Technol.,Cambridge, MA, USA, Tech. Rep. MITCSAIL-TR-2006-014, 2006.

[39] L. Jamone, L. Natale, G. Metta and G. Sandini, "Highly sensitive soft tactile sensor for an anthropomorphic robot hand," *IEEE sensors Journal*, vol. 15, no. 8, pp. 4226-4233, 2015.

[40] L. Jamone, F. Nori, G. Metta, and G. Sandini, "James: A humanoid robot acting over an unstructured world," *in Proc. 6th IEEE-RAS Int. Conf. Humanoid Robots*, pp. 143-150, 2006.

[41] S. Youssefian, N. Rahbar and E. Torres-Jara, "Contact behavior of soft spherical tactile sensor," *IEEE sensors Journal*, vol. 14, no. 5, pp. 1435-1442, 2014.

[42] J.D. Jackson, "Classical Electrodynamics," 3rd edition, Wiley, 1998.

[43] D. S. Chathuranga, Z. Wang, Y. Noh, T. Nanayakkara and S. Hirai, "Robust Real time Material Classification Using Soft Embodied 3D Tactile Sensor," *IEEE Int. Con. on Intelligent Robots and Systems*, 2015.

[44] Q. Liang, D. Zhang,Y. Ge, and Q. Song, "A novel miniature four-dimensional force/torque sensor with overload protection mechanism," *IEEE Sensors Journal*, vol.9, No. 12, pp. 1741-1747, 2009.

[45] I. Kao, and F. Yang, "Stiffness and contact mechanics for soft fingers in grasping and manipulation," *IEEE Transactions on Robotics and Automation*, vol. 20, No. 1, pp. 132-135, 2004.

[46] T. Maeder, V. Fahrny, S. Stauss, G. Corradini and P. Ryser , "Design and characterisation of low-cost thick-film piezoresistive force sensors for the 100 mN to 100 N range," *XXIX International Conference of IMAPS Poland Chapter*, 2005.

[47] Y. L. Park, K. Chau, R. J. Black, and M. R. Cutkosky , "Force Sensing Robot Fingers using Embedded Fiber Bragg Grating Sensors and Shape Deposition Manufacturing," *IEEE International Conference on Robotics and Automation*, pp. 1510-1516, 2007.

[48] P. Polygerinos, L. D. Senevirathne, R. Razavi, T. Schaeffter and K. Althoefer , "Triaxial catheter-tip force sensor for MRI- guided cardiac procedures," *IEEE/ASME Transactions on Mechatronics*, vol. 18, no. 1, pp. 386-396, 2013.

[49] V. A. Ho, D. V. Dao, S. Sugiyama and S. Hirai, "Development and analysis of a sliding tactile soft fingertip embedded with a microforce/moment sensor," *IEEE Transactions on Robotics*, vol. 27, no. 3, pp. 411-424, 2011.

[50] Y. Zhang, A. W. Allen, J. Yi, and T. Liu, "Understanding Tire/Road Stick-Slip Interactions with Embedded Rubber Force Sensors," *IEEE International conference on Advanced Intelligent Mechatronics*, pp. 550-555, 2012.

Damith Suresh Chathuranga received a B.S. degree in Mechanical Engineering from the University of Moratuwa, Sri Lanka, in 2009, and an M.S. in robotics from Ritsumeikan University, Kyoto, Japan, in 2013. He is currently studying for a PhD in Robotics at Ritsumeikan University. He was a visiting researcher at Kings College London, UK in 2014. His current research interests include humanoid robotics, anthropomorphic hands, soft-fingered manipulation, haptics for bio-medical applications and tactile sensors.

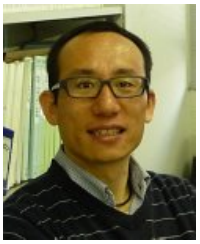

Zhongkui Wang received his Ph.D. degree in science and engineering from Ritsumeikan University, Japan, in 2011. He was a research associate at the department of Robotics, Ritsumeikan University, 2011-2012; a postdoctoral research fellow in the same department from 2012-2014; an academic guest at the Institute of Robotics and Intelligent Systems (IRIS) in Swiss Federal Institutes of Technology, Zurich (ETHz), Switzerland, Sept. 2012-March 2013. He is currently an assistant professor at the department of robotics, Ritsumeikan University, Japan. His research interests include finite element modeling and simulation for medical and nursing applications, optimization-based parameter estimation, tactile sensing and perception, medical instrument development for in vivo measurements, and robotics for food engineering. He is a member of IEEE and JSMBE.

Yohan Noh is a research associate in the Center for Robotics Research (CoRe). He received B.S. degree in the Department of Mechanical Engineering from Seoul National University of Science and Technology, Seoul, Korea in 2002, also received B.S. degree in the Department of Electrical Engineering from Yonsei University, Seoul, Korea in 2004, and He received M.S. and Ph.D. degrees in the Department of Science and Engineering from Waseda University, Tokyo, Japan in 2007 and in 2011 respectively. His research interests include development of force and tactile sensor, haptic devices, torque sensor, force and torque control, medical training system, smart surgical devices, and smart medical devices. Currently, He is a member of IEEE, and RSJ (Robot society of Japan).

Thrishantha Nanayakkara received the BSc and MSc degrees in electrical engineering from the University of Moratuwa (UM), Sri Lanka (1996), and Saga University (SU), Japan (1998), and PhD in robotics from SU (2001). He was a postdoctoral research fellow in the department of biomedical engineering, Johns Hopkins University, USA, 2001-2003; a senior lecturer in the faculty of engineering at the UM; a Radcliffe Fellow at Harvard University, USA (2008/09), and a research affiliate at MIT (2008/09), USA. He is currently a senior lecturer in the department of Informatics, Kings College London. His research interests are in soft robotics, and robotic interaction with uncertain environments. He has published one textbook and more than 80 peer reviewed papers.

Shinichi Hirai received his B.S., M.S., and Doctoral degrees in applied mathematics and physics from Kyoto University in 1985, 1987, and 1991, respectively. He is currently a Professor in the Department of Robotics at Ritsumeikan University. He was a Visiting Researcher at Massachusetts Institute of Technology in 1989 and was an Assistant Professor at Osaka University from 1990 to 1996. His current research interests are modeling and control of deformable objects, realtime computer vision, and softfingered manipulation. He received SICE (Society of Instrument and Control Engineers) Best Paper Award at 1990, JSME (Japan Society of Mechanical Engineers) Robotics and Mechatronics Div. Achievement Awards at 1996, the finalist of Automation Best Paper Award at 2001 IEEE Int. Conf. on Robotics and Automation, the finalist of Manipulation Best Paper Award at 2005 and 2006 IEEE Int. Conf. on Robotics and Automation, the finalist of Vision Best Paper Award at 2006 IEEE Int. Conf. on Robotics and Automation, and RSJ (Robotics Society of Japan) Best Paper Award at 2008. He is serving as an Associate Editor of IEEE Transactions on Robotics from July 2006. He is a member of IEEE, RSJ, JSME, and SICE.